CHEMISTRY
A European Journal

A Journal of
ChemPubSoc Europe

Accepted Article

Title: Reactivity of a Sterically Unencumbered α-Borylated Phosphorus Ylide Towards Small Molecules

Authors: Michael Radius, Ewald Sattler, Helga Berberich, and Frank Breher

To be cited as: *Chem. Eur. J.* 10.1002/chem.201902681

Link to VoR: http://dx.doi.org/10.1002/chem.201902681

Supported by
ACES

WILEY-VCH

Reactivity of a Sterically Unencumbered α-Borylated Phosphorus Ylide Towards Small Molecules

Michael Radius,[a] Ewald Sattler,[a] Helga Berberich,[a] and Frank Breher*[a]

Abstract: The influence of the substituents on α-borylated phosphorus ylides (α-BCPs) has been investigated in a combined experimental and quantum chemical approach. The synthesis and characterization of $Me_3PC(H)B(iBu)_2$ (**1**) consisting of small Me substituents on phosphorous and *i*Bu residues on boron is reported. **1** is accessible in a novel synthetic approach, which was further elucidated by density functional theory (DFT) studies. The reactivity of **1** towards various small molecules was probed and compared with the previously published derivative $Ph_3PC(Me)BEt_2$ (**2**). Both α-BCPs react with NH_3 to undergo heterolytic N–H bond cleavage. Different dimeric and trimeric ring structures were observed in the reaction products of **1** with CO (**3**) and CO_2 (**4**). With PhNCO and PHNCS, the expected insertion products $[Me_3PC(H)(PhNCO)B(iBu)_2]$ (**5**) and $[Me_3PC(H)(PhNCO)B(iBu)_2]$ (**6**) were isolated.

Introduction

Since the discovery of the activation of dihydrogen by a main group element compound by Power *et al.* in 2005,[1] and the reversible cleavage of dihydrogen by Stephan *et al.* in 2006,[2] the field of main group element-based molecules mimicking transition metal chemistry – e.g. small molecule activation – is quickly developing.[3] The most prominent group of compounds are the so called “frustrated Lewis pairs” (FLPs) in which a Lewis acid and a Lewis base are hindered of combining inter- or intramolecularily.[4] However, FLP-type reactivity is not only observed for unquenched Lewis pairs. For instance, carbenes inherently featuring ambiphilic character are also able to react with e.g. H_2 or NH_3.[5] Heteroalkenes possessing perturbed element element double bonds also show FLP-type reactivity towards small molecules.[6] Stephan *et al.* reported already in 2008 on the addition of H_2 to a phosphinoborane (Scheme 1).[6h] Recently, it has been demonstrated that conjugated, boron substituted multiple bonds show ambiphilic reactivity.[7] In this line of thought, Stephan and Erker lately pointed out that “borate alkenes can be viewed as FLPs with adjacent donor and acceptor sites”.[4e, 8] Our group recently reported on an α-borylated phosphorus ylide (α-BCP)[9] featuring a highly polarized borata alkene subunit.[10a] We found that the α-BCP readily reacts with CO, CO_2, COS, CS_2, PhNCO and PhNCS (Scheme 1).[10a] In order to probe whether the reactivity of α-BCPs can be modified by changing the substituent pattern, we became interested to study α-BCPs with small Me substituents on the phosphorus atom.

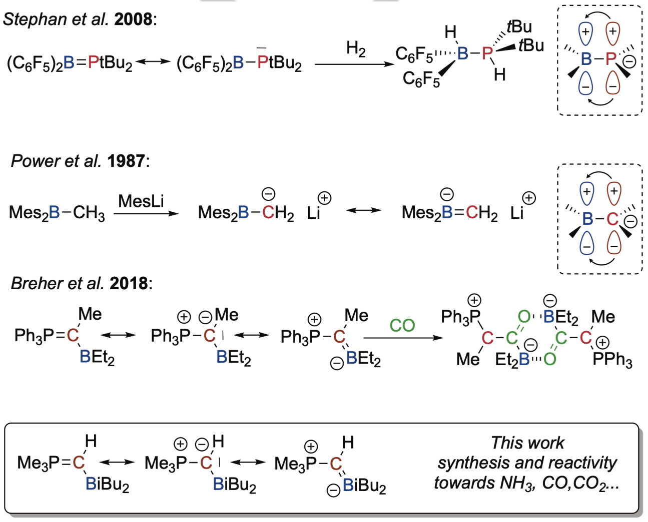

Scheme 1. Structure and reactivity of selected heteroalkenes.

Results and Discussion

We first targeted the smallest possible α-BCP, that is the all-Me substituted derivative $Me_3PC(H)BMe_2$. However, transylidation[11] of $Me_3PC(H)_2B(Br)Me_2$ with Me_3PCH_2 did not lead to the desired target structure, at least in our hands. The main product of the reaction was found to be the eight-membered ring $[H_2C–PMe_2–CH_2–BMe_2]_2$. During our studies on phosphorous ylides we found by chance that the reaction of $iBu_2B–P(tBu)_2$ with Me_3PCH_2 yields $Me_3PC(H)B(iBu)_2$ (**1**, Scheme 2). The starting material $iBu_2B–P(tBu)_2$ was generated *in situ* in order to prevent isobutene elimination. The expected intermediate was isolated and we successfully obtained NMR spectroscopic evidence for the four-membered PC_2B ring structure, which is known from the literature.[12] The NMR measurement was conducted in toluene-d_8 at -60 °C. The $^{31}P\{^1H\}$ resonance is detected at $\delta = 27.6$ ppm, shifted about 25 ppm downfield compared to **1**. The ^{11}B NMR resonance with a chemical shift of $\delta = –10.9$ ppm is about 60 ppm upfield compared to **1**. Overall, the chemical shifts fit perfectly to the inner salt character of the four-membered ring structure. The ^1H NMR resonances are detected at $\delta = 0.60$ ppm ($^2J_{PH} = 13.1$ Hz, 6H) for the hydrogen atoms of the P-bound methyl groups and at 0.43 ppm ($^2J_{PH} = 14.6$ Hz, 4H) for the bridging CH_2 groups. The couplings collapse if the ^1H NMR spectrum is recorded with ^{31}P

---

[a] M.Sc. M. Radius, Dr. E. Sattler, H. Berberich, Prof. Dr. F. Breher
Institute of Inorganic Chemistry, Division Molecular Chemistry
Karlsruhe Institute of Technology (KIT)
Engesserstr. 15, 76131 Karlsruhe (Germany)
E-mail: breher@kit.edu

Supporting information and the ORCID identification number(s) for the author(s) of this article can be found under:
https ://doi.org/10.1002/chem.xxx

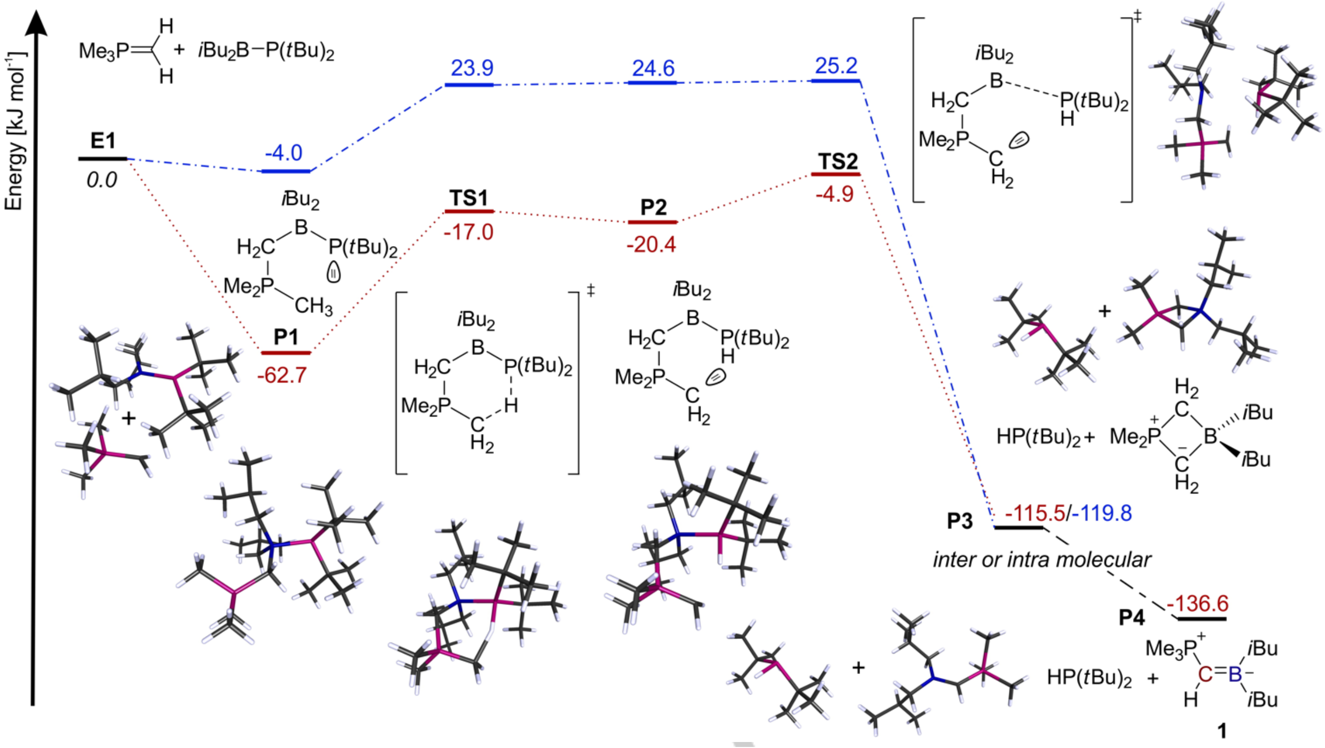

Figure 1. Calculated [BP86/(ri-)def2-SVP] reaction pathway, electronic energies (in red) and Gibbs free energies (in blue) to **1**. The free energies are calculated at 233.15 K.

decoupling. We note in passing that the ^{1}H NMR resonances of the *i*Bu substituents are not perfectly isochrone, probably due to the possible *endo/exo* positions (cf. the structure of the quantum chemical calculation).

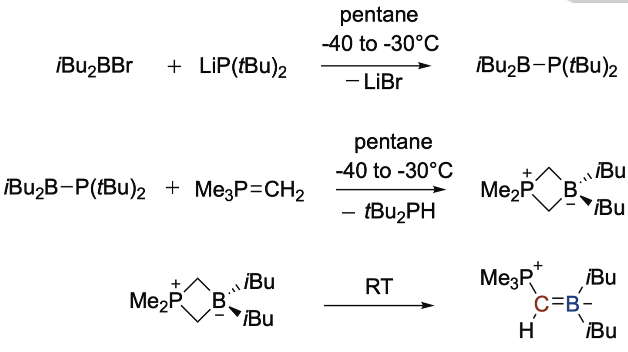

1

Scheme 2. Synthesis of **1**.

Since ylides are very strong σ-donors,[13] an initial coordination to the Lewis acidic boron atom of *i*Bu$_2$B–P(*t*Bu)$_2$ is very likely. In order to shed some light on the reaction mechanisms for the formation of **1**, we calculated the reaction pathway of the deprotonation of Me$_3$P=CH$_2$ and the formation of a four-membered ring (Figure 1). The Gibbs free energy for the coordination of the ylide to the boron atom and formation of **P1** is slightly exergonic (–4 kJ mol^{-1}, Figure 1). The energy barrier to the six-membered ring that comprises the transition state for the proton shift from the methyl group to the phosphorus atom (product **P2**) was found to be only 27.9 kJ mol^{-1} and, thus, quite low. The subsequent dissociation of *t*Bu$_2$PH is nearly without an energy barrier. The formations of the PC$_2$B four-membered ring compound **P3** and the open α-BCP structure **P4** (i.e. **1**) are both highly exergonic (–119.8 and –136.6 kJ mol^{-1}, respectively). The rearrangement to the α-BCP **1** can proceed either inter- or intramolecularly. Overall, these calculated Gibbs free energies are in good agreement with the reaction conditions.

Further quantum chemical calculations revealed a very similar electron distribution for **1** as compared to the previously reported derivative Ph$_3$PC(Me)BEt$_2$ (**2**).[10a] The calculated frontier orbitals are depicted in Figure 2 showing the HOMO to comprise mainly of the p-type C-based lone pair of electrons with a smaller coefficient on the boron atom. The LUMO mainly comprises of the vacant p orbital on boron and partly the antibonding P–C$_{Me}$ orbitals.

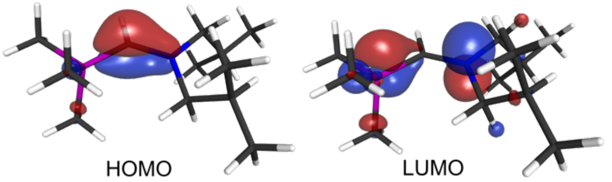

Figure 2. Kohn-Sham HOMO and LUMO of **1** (BP86/def2-TZVPP, isosurface value of 0.06).

As for **2**, we calculated the fluoride ion affinity (FIA)[14] of **1** (BP86/def2-SVP). The FIA of **1** was found to amount to 196 kJ mol^{-1}, i.e. ca. 30 kJ mol^{-1} lower than **2** (224 kJ mol^{-1}). The main difference in the electronic structure is caused by the substitution of the C_{ylide}-hydrogen in **1** by the CH_3 group in **2**. This becomes clear when the charges of the natural population analysis are compared. To this end, we calculated the charges for the model compounds **q1^{H}**, **q2^{Me}** and the hypothetical molecules **q1^{Me}** and **q2^{H}** with Me and H substituents on the ylidic carbon atoms, respectively (Scheme 3).

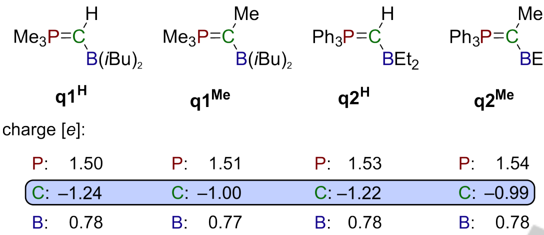

Scheme 3. Natural population analysis charges (BP86/def2-SVP) of **q1^{H}**, **q1^{Me}**, **q2^{H}** and **q2^{Me}**.

Although the charges on the boron and phosphorus atoms do not change significantly, the charges on the ylidic carbon atoms for the model compounds bearing a C_{ylide}–H bond (**q1^{H}**, **q2^{H}**) are more negative (–0.25 e) than for the two methylated analogous **q1^{Me}** and **q2^{Me}**. It appears that this higher charge density is partly responsible for the lower FIA calculated for **1** and has its origin in the inability of the H-substituent to participate in negative hyperconjugation. Nevertheless, the higher charge is not reflected in the Wiberg bond indices (WBI). The WBIs of the P–C_{ylide} and the C_{ylide}–B bonds in **1** are calculated to amount to 1.28 and 1.41, respectively, and are thus very similar to **2** (P–C_{ylide}: 1.25, C_{ylide}–B: 1.42).[10a]

To further elucidate the influence of the other B- and P-bound substituents, we calculated the FIA for several additional model compounds (**qR^{1}R^{2}** with R^{1} bound to the phosphorus atom and R^{2} bound to the boron atom; R^{1}/R^{2} = Me, Et, *i*Pr, Ph; Table 1). From this study it becomes clear that for small alkyl substituents such as Me on boron the FIA is obviously reduced (hyperconjugative effects). A further increase of the degree of alkylation upon going from **qMeMe** to **qMeEt** to **qMePr** gradually increases the FIA from 171 to 195 to 219 kJ mol^{-1}, respectively. Aryl groups such as Ph further increase the FIA to 229 kJ mol^{-1} (*cf.* **qMePh**, entry 4). The highest FIA was found for the all-Ph derivative **qPhPh** (entry 8, 258 kJ mol^{-1}). Also, the influence of the substituents on the phosphorus atom is significant. This may be due to the higher Lewis acidity of the PR$^{1}_{3}$ fragment because of lowering of the σ*(P–C) orbitals. These trends correlate well with the group electronegativity (increasing from Me via Et and *i*Pr to Ph) of the substituents.[15] Interestingly, the calculated C–B bond lengths remain almost the same for the whole series of model compounds.

Table 1. Calculated [BP86/def2-SV(P)] fluoride ion affinity (FIA) and C–B bond lengths for different model compounds.

Entry	Compound	FIA	*d*(C–B) [pm]
1	$Me_3PC(Me)BMe_2$ (**qMeMe**)	165	151.0
2	$Me_3PC(Me)BEt_2$ (**qMeEt**)	197	150.8
3	$Me_3PC(Me)B(i\text{Pr})_2$ (**qMePr**)	221	151.5
4	$Me_3PC(Me)BPh_2$ (**qMePh**)	220	150.3
5	$Et_3PC(Me)BMe_2$ (**qEtMe**)	181	151.1
6	$i\text{Pr}_3PC(Me)BMe_2$ (**qPrMe**)	196	151.4
7	$Ph_3PC(Me)BMe_2$ (**qPhMe**)	226	151.6
8	$Ph_3PC(Me)BPh_2$ (**qPhPh**)	267	150.8

In order to probe the reactivity of **1**, we performed reactions with various small molecules. As with $Ph_3PC(Me)BEt_2$,[10a] **1** does not react with dihydrogen but the reaction with NH_3 possessing a relatively strong N–H bond (*D* = 446 kJ mol^{-1}),[16] smoothly proceeds at room temperature with both ylides **1** and **2**. The corresponding ylide and the amidoborane $R_2B–NH_2$ are formed (Scheme 4), as evidenced by ^{11}B and ^{31}P NMR spectroscopic investigations. The ^{31}P{^{1}H} NMR chemical shifts clearly indicate the formation of the ylides. The ^{11}B NMR resonances are shifted upfield from 56.5 to 48.7 ppm for **2** and from 54.7 ppm to 47.6 ppm for **1**, respectively, perfectly matching literature values for $R_2B–NH_2$.[17]

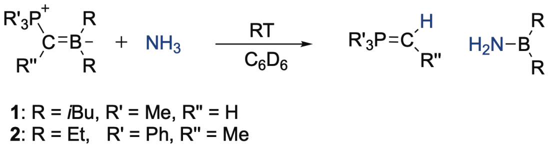

Scheme 4. Reaction of **1** and **2** with NH_3 at room temperature.

It has to be noted that precedents for such a reactivity have been published before for dialkyl boron compounds. The splitting of NH_3 under formation of $R_2B–NH_2$ takes place in boron compounds featuring Lewis basic substituents such as $R_2B–SEt$ or with *t*BuC(O)O–BEt_2.[18]

1 reacts at elevated temperatures with CO in toluene. However, the structure of the product (**3**) differs from that found for **2**. While the latter forms a dimeric structure (Scheme 5), **1** forms an adduct with another equivalent of α-BCP.

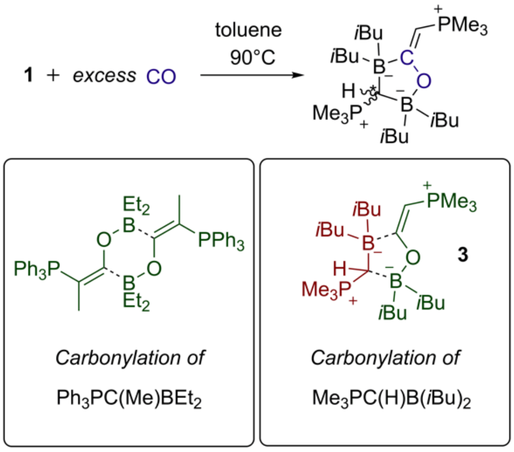

Scheme 5. Reaction of **1** with CO to **3** and comparison with the reactivity found for **2**.[10a]

Single crystals of **3** suitable for X-ray diffraction studies were obtained from hexane solution at room temperature (Figure 3). The space group for **3** was found to be $P2_1/c$ and since **3** comprises a stereocenter at C2, both enantiomers are present in the solid state. The core structure is composed of a five-membered C_2OB_2 heterocycle with C2 residing ca. 15° above the plane spanned by the atoms B2, C3, O1 and B1. The P2–C2 bond length of 1.716 Å falls in the typical range for stabilized ylidic bonds.[10a] The analogous P1–C1 bond (1.742 Å) is slightly elongated. As expected, the distances C1–C3 (1.404 Å) and C3–O1 (1.329 Å) fall in between typical single and double bond lengths. The carbon–boron bond lengths are in the expected range.

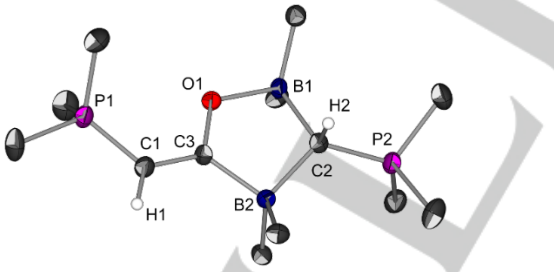

3

Figure 3. ORTEP view (30% probability ellipsoids) of **3**. Hydrogen atoms (except H1 and H2) and the C(H)Me_2 part of the *i*Bu groups are omitted for clarity. Only the main part of the disordered structure is depicted. Selected bond lengths (Å) and angles (°): P1–C1 1.716(5), P2–C2 1.742(4), C1–C3 1.404(8), C3–O1 1.329(7), C3–B2 1.625(7), C2–B2 1.689(6), C2–B1 1.673(5), B1–O1 1.556(5), C3–C1–P1 121.7, O1–C3–C1 114.4(5), C1–C3–B2 129.2(5), B1–C2–B2 105.7(3).

The ylidic carbon atom C1 adopts a trigonal planar coordination environment in the crystal structure. However, as Mitzel *et al.* reported,[19] the solid-state structure is not always representative for the local geometry of an ylidic carbon atom in solution or the gas phase. Indeed, we detected in solution two well-separated chemical shifts for H1 and P2 in the ^{1}H and ^{31}P NMR spectrum, respectively, both integrating 1:1 (Figure 4). This can most likely be attributed to the presence of two diastereomers, *i.e.* a second stereocenter besides the one at C2 depicted in Figure 4. This suggests that the local geometry of the ylidic carbon atom is not planar but (slightly) pyramidal,[20] thus providing a second stereocenter at C1. Interchange of one diastereomer into another *via* pyramidal inversion at C1 leads naturally to the uniformly distributed intensities (1:1).[21]

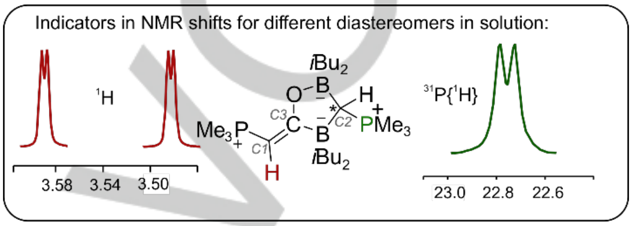

Figure 4. Sections of the ^{1}H and ^{31}P{^{1}H} NMR spectra of **3**. Atom numbering in the schematic drawing according to Figure 3.

The different reactivity of **1** towards CO as compared to **2** may at least in part be explained by the lower FIA of **1**. Quantum chemical calculations predicted the insertion/ylide adduct **3** to be 38 kJ mol^{-1} more stable than the hypothetical dimeric insertion product found for **2**.

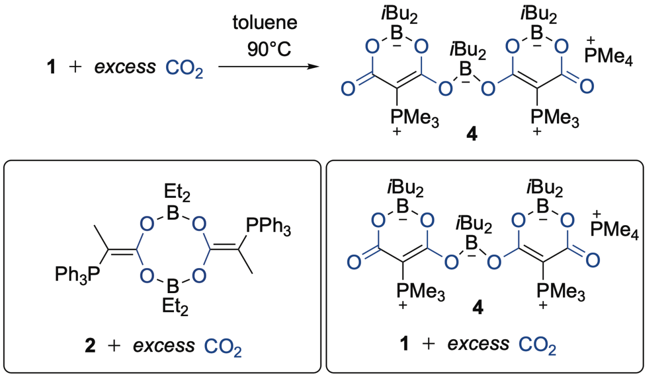

Scheme 6. Reaction of **1** with CO_2 to **4** and comparison with the reactivity found for **2**.

The reactivity of **1** towards CO_2 has also been investigated. Again, the product (**4**) differs considerably from the product observed for **2** with CO_2 (Scheme 6). Interestingly, the reaction product is formed by three α-BCPs and four CO_2 molecules. Two molecules of **1** directly react with CO_2, each of which with two molecules of CO_2. Six-membered ring structures of the insertion products are formed, both of which are deprotonated by the third molecule of **1** forming $[PMe_4]^+$ and a $\{B(i\text{Bu})_2\}^+$ fragment. The latter is attached to the newly formed six-membered rings furnishing an overall negatively charged borate. Thus, as in the reaction product of **2** with CO_2, the boron atoms are saturated by binding to two oxygen atoms. In the reaction of **2** with CO_2, however, the methyl group inhibits further reaction like the one displayed by **1**.

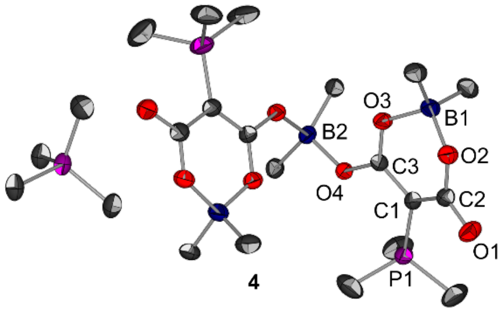

Figure 5. ORTEP view (30% probability ellipsoids) of **4**. Hydrogen atoms and the C(H)Me_2 part of the *i*Bu groups are omitted for clarity. Only the main part of the disordered structure is depicted. Selected bond lengths (Å) and angles (°) (The structural parameters of only one half of the anion is given since the second half is metrically similar.): P1–C1 1.74(1), C1–C2 1.439(3), C1–C3 1.406(3), C2–O1 1.241(2), C2–O2 1.304(2), C3–O3 1.284(2), C3–O4 1.288(2), B1–O2 1.520(3), B1–O3 1.539(3), B2–O4 1.546(2), C2–C1–C3 120.2(2).

Single crystals of **4** suitable for X-ray diffraction studies were obtained from toluene at room temperature (space group P-1, Figure 5). The structural parameters of only one half of the anion is discussed since the second half is metrically similar. The Me_4P^+ cation shows the expected structural parameters.[22] Although the C1–C2 bond length of 1.439 Å is slightly longer than the corresponding C1–C3 bond of 1.406 Å, both still adopt values between C–C single and double bonds. The carbon oxygen distances range from 1.241 Å for C2–O1 to 1.304 Å for C2–O2. The phosphorous carbon bond length P1–C1 (1.744 Å) indicates a small ylidic contribution. All B–O distances are in the expected range.[23]

The NMR spectroscopic characterization fully supported the structure of **4** found in the solid state. For instance, two well-separated ^{13}C NMR chemical shifts are found for the C<u>C</u>O₂ entities at δ = 174.0 and 171.8 ppm. In the ^{11}B NMR spectrum only one broad resonance is detected at δ = –14.9 ppm. Although the bridging boron moiety (B2) and the boron moieties in the six membered rings possess slightly distinct environments, the differences are probably not significant enough to cause to furnish two distinct ^{11}B NMR shifts.

The α-BCP **1** reacts also with PhNCO and PhNCS. The reaction products are analogous to the ones observed for **2**. In each case, one PhNCX molecule inserts into the C_{ylidic}–B bond of one α-BCP and the boron atom is chelated by the nitrogen and the chalcogen atoms (Scheme 7).[10a]

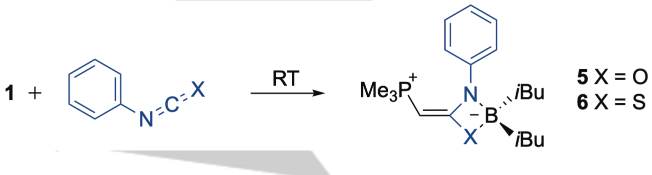

Scheme 7. Reaction of **1** with PhNCO and PhNCS to **5** and **6**.

We note in passing that the reaction products **5** and **6** thermally decompose easily. In the case of **5**, above *ca.* 60 °C, and in the case of **6** at slightly higher temperatures at 89 °C. This may be due to the higher ring strain in the small NBOC four-membered ring of **5** as compared to the widened NBSC ring of **6**.

Single crystals of **5** (space group $P2_1/n$) and **6** (space group P-1) suitable for X-Ray diffraction studies were obtained from benzene toluene/pentane, respectively. The molecular structures are depicted in Figure 6 and the bond lengths and angles are very similar to published values. An interesting structural feature of **6** is the exceptional long B1–S1 bond length of 2.082 Å, which indicates the formation of a weak B1···S1 contact instead of a strong bond. The corresponding bond length B1–O1 in **5** (1.593 Å) is slightly elongated compared to the boron oxygen bonds in **3** and **4** (1.54 – 1.56 Å). These structural features, together with the low decomposition temperature, clearly support the view of strained four-membered rings. The NMR spectra of **5** and **6** are very similar (see Experimental Section).

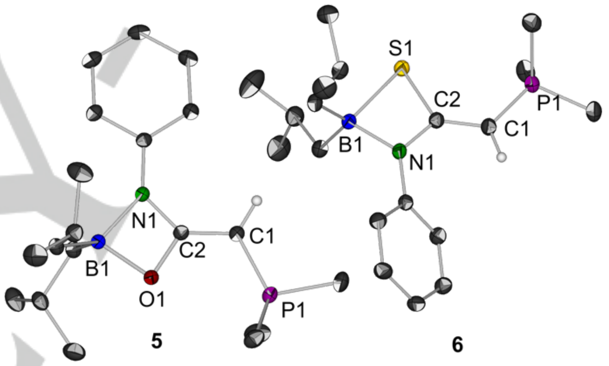

Figure 6. ORTEP view (30% probability ellipsoids) of **5** and **6**. Hydrogen atoms (except the ylidic) are omitted for clarity. Selected bond lengths (Å) and angles (°): **5**: P1–C1 1.723(2), C1–C2 1.376(2), N1–C2 1.353(2), O1–C2 1.331(2), N1–B1 1.603(2), O1–B1 1.593(2), P1–C1–C2 119.2(1), N1–C2–O1 101.3(1), C2–N1–B1 88.0(1), C2–O1–B1 89.2(1), N1–B1–O1 81.0(1). **6**: P1–C1 1.720(2), C1–C2 1.378(3), N1–C2 1.349(2), S1–C2 1.752(2), N1–B1 1.585(3), S1–B1 2.082(2), P1–C1–C2 124.58(15), N1–C2–S1 102.5(1), C2–N1–B1 102.6(1), C2–S1–B1 72.92(8), N1–B1–S1 81.9(1).

Conclusions

In conclusion, we note that the fundamental reactivity of an α-BCP is untouched by the substitution of the P-bound phenyl groups by methyl groups and reactions occur with NH_3, CO, CO_2, PhNCO and PhNCS. However, in the case of CO and CO_2, different products and structures are observed for $Me_3PC(H)B(iBu)_2$ (**1**) as compared to the previously published derivative $Ph_3PC(Me)BEt_2$ (**2**). In part, the different reaction patterns can be explained by different fluoride ion affinities of both α-BCPs. Nevertheless, also the presence of a C_{ylide}–H bond in **1** is responsible for secondary reactions arising from this reactive functional group.

Experimental Section

All operations were conducted under a dry argon atmosphere using standard Schlenk and glovebox techniques. Solvents were dried rigorously and degassed before use. $Me_3P{=}CH_2$,[24] iBu_2BCl[25] and $LiP(tBu)_2$[26] were synthesized according to literature procedures. The chemical shifts are expressed in parts per millions and ^{1}H and ^{13}C signals are given relative to TMS. Coupling constants J are given in Hertz as positive values regardless of their real individual signs. The multiplicity of the signals is indicated as s, d, q, sept or m for singlets, doublets, quartets, septets or multiplets, respectively. The assignments were confirmed as necessary with the use of 2D NMR correlation experiments. Mass spectrometry measurements were performed on an Advion expression^{L} CMS mass spectrometer under atomic pressure chemical ionization (APCI). IR spectra were measured with a Bruker Alpha spectrometer using the attenuated total reflection (ATR) technique on powdered samples, and the data are quoted in wavenumbers (cm^{-1}). The intensity of the absorption band is indicated as vw (very weak), w (weak), m (medium), s (strong), vs. (very strong) and br (broad). Melting points were measured with a Thermo Fischer melting point apparatus and are not corrected. Elemental analyses were carried out in the institutional technical laboratories of the Karlsruhe Institute of Technology (KIT).

Synthesis of 1. To a solution of iBu_2BCl (7.67 g, 47.8 mmol) in 200 ml pentane was slowly added a suspension of $LiP(tBu)_2$ (7.61 g, 50.0 mmol) in 200 ml pentane at –50 °C. After stirring the suspension at –40 °C for 48 hours the suspension was filtered in the cold and washed with cold pentane. The residue was extracted with cold toluene. At –50 °C to this solution was added a solution of $Me_3P{=}CH_2$ (1.85 g, 20.5 mmol) in 50 ml pentane. White precipitate formed. After cold filtration the precipitate was washed with cold pentane. (From this precipitate, the NMR spectra of $Me_2P(CH_2)_2B(iBu)_2$ were measured.) At room temperature, the solid turned liquid. Distillation at high vacuum ($p = 3 \cdot 10^{-6}$ bar) at 20 °C yields **1** (2.01 g, 9.39 mmol, 52%): ^{1}H NMR (300 MHz, C_6D_6, ppm): δ = 2.36 (d, $^{2}J_{PH}$ = 12.1 Hz, H_{ylid}, 1H), 2.26 (nonet, $^{3}J_{HH}$ = 6.7 Hz, H_{iBuCH}, 2H), 2.21 (nonet, $^{3}J_{HH}$ = 6.7 Hz, H_{iBuCH}, 2H), 1.28 (d, $^{3}J_{HH}$ = 6.8 Hz, H_{iBuCH2}, 2H), 1.27 (d, $^{3}J_{HH}$ = 6.5 Hz, H_{iBuCH3}, 6H), 1.16 (d, $^{3}J_{HH}$ = 6.5 Hz, H_{iBuCH3}, 6H), 1.12 (d, $^{3}J_{HH}$ = 7.2 Hz, H_{iBuCH2}, 1H), 1.12 (d, $^{3}J_{HH}$ = 7.2 Hz, H_{iBuCH2}, 1H), 0.86 (d, $^{2}J_{PH}$ = 12.6 Hz, H_{PMe3}, 9H); ^{11}B-NMR (96 MHz, C_6D_6, ppm): δ = 54.7 (s); $^{13}C\{^{1}H\}$ NMR (75 MHz, C_6D_6, ppm): δ = 48.5 (bs, C_{ylid}), 37.2 (bs, C_{iBuCH2}), 36.0 (bs, C_{iBuCH2}), 27.3 (s, C_{iBuCH1}), 27.3 (s, C_{iBuCH1}), 26.7 (s, C_{iBuCH3}), 26.7 (s, C_{iBuCH2}), 17.6 (d, $^{1}J_{PC}$ = 56.2 Hz, C_{PMe3}); $^{31}P\{^{1}H\}$ NMR (121 MHz, C_6D_6, ppm): δ = 2.03 (s); EI-MS: 214.20214, $C_{12}H_{28}{}^{11}BP$, calc. 214.20216; elemental analysis (%): $C_{12}H_{28}BP$ calc. P, 14.46, B, 5.05 found P, 14.40, B, 5.08; cryoscopy (benzene, g mol^{-1}): calc. 214.14, found 212.0; IR (ATR, cm^{-1}): ũ = 2944 (m), 2891 (w), 2860 (m), 1461 (w), 1419 (w), 1375 (m), 1347 (vs), 1315 (s), 1289 (m), 1250 (w), 1207 (vw), 1155 (w), 1091 (vw), 1056 (vw), 1034 (vw), 980 (s), 936 (s), 890 (w), 858 (w), 816 (w), 750 (w), 731 (m), 697 (w), 647 (vw), 577 (vw), 500 (vw), 412 (vw).

Synthesis of 3: A Schlenk tube with a solution of 0.864 g (1.00 ml, 4.03 mmol) **1** in 10 ml toluene was degassed with two freeze-pump-thaw cycles and subsequently purged with CO. The reaction mixture was stirred and heated to 70 °C for three hours. The solution was evaporated to dryness. Pentane (20 ml) was added to the residue, yielding a thin suspension. The suspension was filtered. The filtrate was reduced until crude **3** precipitates. Recrystallisation in boiling pentane, taking of the supernatant layer and drying in high vacuum yielded 250 mg (0.548 mmol, 14 %) pure **3** (both diastereomers) as colourless crystals. Suitable crystals for X-ray diffraction were obtained by solving **3** in a small amount of boiling hexane and cooling the solution very slowly to room temperature: ^{1}H NMR (signal assignment where necessary with $^{1}H\{^{11}B\}$) (300 MHz, C_6D_6, ppm): δ = 3.54 (d, $^{2}J_{PH}$ = 32.1 Hz, $H_{diastereomer1\_C=C}$, 0.5H), 3.53 (d, $^{2}J_{PH}$ = 32.1 Hz, $H_{diastereomer2\_C=C}$, 0.5H), 2.35-2.17 (m, H_{iBuCH1}, 2H), 2.04-1.82 (m, H_{iBuCH1}, 2H), 1.46 (d, $^{3}J_{HH}$ = 6.5 Hz, H_{iBuCH3}, 3H) , 1.43 (d, $^{3}J_{HH}$ = 6.6 Hz, H_{iBuCH3}, 3H), 1.37 (d, $^{3}J_{HH}$ = 6.6 Hz, H_{iBuCH3}, 3H), 1.37 (d, $^{3}J_{HH}$ = 6.6 Hz, H_{iBuCH3}, 3H), 1.34 (d, $^{3}J_{HH}$ = 6.6 Hz, H_{iBuCH3}, 3H), 1.29 (d, $^{3}J_{HH}$ = 6.5 Hz, H_{iBuCH3}, 3H), 1.29 (d, $^{3}J_{HH}$ = 6.5 Hz, H_{iBuCH3}, 3H), 1.28 (d, $^{3}J_{HH}$ = 6.5 Hz, H_{iBuCH3}, 3H), 1.14 (dd, $^{2}J_{HH}$ = 14.2 Hz, $^{3}J_{HH}$ = 7.5 Hz, H_{iBuCH2}, 1H), 1.08 (dd, $^{2}J_{HH}$ = 13.7 Hz, $^{3}J_{HH}$ = 5.5 Hz, H_{iBuCH2}, 1H), 1.00 (d, $^{2}J_{PH}$ = 12.5 Hz, H_{BCPMe3}, 9H), 0.92 (dd, $^{2}J_{HH}$ = 12.5 Hz, $^{3}J_{HH}$ = 5.1 Hz, H_{iBuCH2}, 1H), 0.85 (dd, $^{2}J_{HH}$ = 12.9 Hz, $^{3}J_{HH}$ = 6.1 Hz, H_{iBuCH2}, 1H), 0.89 (d, $^{2}J_{PH}$ = 13.5 Hz, H_{CCPMe3}, 9H), 0.63 (dd, $^{2}J_{HH}$ = 14.1 Hz, $^{3}J_{HH}$ = 3.7 Hz, H_{iBuCH2}, 1H), 0.54 (dd, $^{2}J_{HH}$ = 14.2 Hz, $^{3}J_{HH}$ = 4.7 Hz, H_{iBuCH2}, 1H), 0.36 (dd, $^{2}J_{HH}$ = 12.8 Hz, $^{3}J_{HH}$ = 5.0 Hz, H_{iBuCH2}, 1H), 0.32 (d, $^{2}J_{PH}$ = 22.8 Hz, $H_{BC(H)P}$,1H), 0.31 (dd, $^{2}J_{HH}$ = 12.2 Hz, $^{3}J_{HH}$ = 5.1 Hz, H_{iBuCH2}, 1H); ^{11}B NMR (96 MHz, C_6D_6, ppm): δ = 7.2 (bs), –9.4 (s); $^{13}C\{^{1}H\}$ NMR (75 MHz, C_6D_6, ppm): δ = 231.9 (bs, C_{CO}), 59.3 (d, $^{1}J_{CP}$ = 88.2 Hz, C_{PCC}), 40.2 (bs, C_{iBuCH2}), 29.6 (s, C_{iBuCH3}), 29.1 (s, C_{iBuCH3}), 29.0 (s, C_{iBuCH3}), 28.9 (s, C_{iBuCH3}), 28.6 (s, s, C_{iBuCH}), 28.6 (s, C_{iBuCH3}), 27.7 (s, C_{iBuCH3}), 27.0 (s, C_{iBuCH}), 27.0 (s, C_{iBuCH}), 26.9 (s, C_{iBuCH3}), 15.4 (d, $^{1}J_{PC}$ = 52.1 Hz, C_{BCPMe}), 14.6 (bs, C_{BCP}) 12.4 (d, $^{1}J_{PC}$ = 58.0 Hz, C_{CCPMe}); $^{31}P\{^{1}H\}$ NMR (121 MHz, C_6D_6, ppm): δ = 22.8 (s,$P_{diastereomer1\_BCP}$), 22.7 (s, $P_{diastereomer2\_BCP}$), -4.23 (s, P_{CCP}); APCI-MS: decomposition; melting point: 181° C; elemental analysis: $C_{25}H_{56}B_2OP_2$ calc. C 65.81; H 12.37; found. C 65.64; H 12.32; IR (ATR, cm^{-1}): ũ = 2936 (m), 1893 (w), 2850 (s), 2802 (w), 1451 (m), 1437 (s), 1356 (vw), 1331 (w), 1311 (w), 1288 (m), 1242 (w), 1159 (w), 1132 (w), 1107 (m), 1077 (m), 970 (s), 944 (vs), 907 (s), 861 (s), 823 (m), 748 (vs), 718 (s), 691(vs),648 (m), 620 (m), 602 (m), 574 (m), 546 (s), 525 (vs), 497 (s), 485 (s), 469 (m), 459 (m), 449 (m), 440 (m), 430 (s), 421 (s), 410 (m), 401 (m), 392 (m), 382 (m).

4: A solution of 700 mg (3.27 mmol) of **1** in 10 ml toluene was degassed with two freeze-pump-thaw cycles and subsequently purged with 1.1 bar CO_2. The solution was stirred and heated to 90 °C overnight. The solvent and all volatile compounds were evaporated in high vacuum. After removing all volatiles, the crude product was only slightly soluble in toluene. Crude **4** was recrystallized in toluene, yielding after removal of the supernatant layer and drying in high vacuum 538 mg (0.657 mmol, 60 %) colourless crystalline **4**. Crystals suitable for X-ray diffraction were obtained by solving a small amount of **4** in hot toluene and cooling the solution very slowly to room temperature: ^{1}H NMR (300 MHz, THF-d_8, ppm): δ = 2.03 (d, $^{2}J_{PH}$ = 15.2 Hz, H_{PMe3}, 12H), 1.80 (d, $^{2}J_{PH}$ = 14.1 Hz, H_{PMe4}, 18H), 1.76 – 1.65 (m, H_{iBuCH_ring}, 4H) ,1.59 (sept, $^{3}J_{HH}$ = 6.5 Hz, H_{iBuCH_bridge}, 2H), 0.86 (d, J = 6.5 Hz, H_{iBuCH3_ring}, 24H), 0.84 (d, J = 6.5 Hz, H_{iBuCH3_bridge}, 12H), 0.66 (d, J = 6.9 Hz, H_{iBuCH2_bridge}, 4H) 0.28 (bs, H_{iBuCH2_ring}, 8H). ^{11}B NMR (96 MHz, THF-d_8, ppm): δ = –14.9 (bs); $^{13}C\{^{1}H\}$-NMR (101 MHz, THF-d_8, ppm): δ = 174.0 (bs, C_{CO2}), 171.8 (bs, C_{CO2}), 57.5 (d, $^{1}J_{PC}$ = 128 Hz, C_{PCCO}) 35.2 (bs, C_{iBuCH2_ring}), 32.6 (bs, C_{iBuCH2_bridge}), 27.9 (s, C_{iBuCH3_ring}), 27.0 (s, C_{iBuCH3_bridge}), 27.0 (s, C_{iBuCH_bridge}), 26.5 (s, C_{iBuCH_ring}), 13.9 (d, $^{1}J_{PC}$ = 62.0 Hz, C_{PMe3}), 9.9 (d, $^{1}J_{PC}$ = 44.8 Hz, C_{PMe4}); $^{31}P\{^{1}H\}$ NMR (121 MHz, THF-d_8, ppm): δ = 25.7 (s, P_{Me4}), 9.9 (s, P_{ylid}); APCI-MS: decomposition; melting point: 174 °C (decomp.); elemental analysis (%): $C_{40}H_{84}B_3O_8P_3$ calc. C, 58.70, H, 10.35 found C, 58.34, H, 10.73; IR (ATR, cm^{-1}): ũ = 2983 (vw), 2937 (w), 2854 (w), 2792 (vw), 1592 (m), 1579 (m), 1490 (vs), 1452 (vs), 1407 (m), 1373 (vw), 1356 (vw), 1318 (m), 1291 (w), 1245 (m), 1179 (w), 1100 (m), 1058 (w), 982 (s), 964 (s), 947 (s), 898 (w), 865 (w), 840 (m), 816 (w), 789 (m), 756 (m), 729 (vw), 681 (m), 629 (vw), 585 (w), 534 (vw), 506 (vw), 464 (w), 419 (vw), 404 (vw).

5: A solution of 500 mg **1** in 8 ml hexane and a solution of 258 mg (2.16 mmol) PhNCO in 8 ml hexane were combined under stirring at room temperature. Stirring was discontinued and crude **5** crystallised. After one hour reaction time, the supernatant layer was taken off and the colourless crystals were dried in high vacuum. The crude product was solved in benzene and filtered. Evaporation of the solvent and drying in high vacuum yielded 282 mg (0.846 mg, 39 %) pure **5**. Crystals suitable for X-ray diffraction were obtained by slow solvent evaporation of a benzene solution of **5**: ^{1}H NMR (300 MHz, C_6D_6, ppm): δ = 7.28 – 7.26 (m, $H_{ortho/meta}$, 4H), 6.92 – 6.83 (m, H_{para}, 1H), 2.62 (d, $^{2}J_{PH}$ = 18.2 Hz, H_{ylide}, 1H), 2.15 (sept, $^{3}J_{HH}$ = 6.6 Hz, H_{iBuCH}, 2H), 1.29 (d, $^{3}J_{HH}$ = 6.6 Hz, H_{iBuCH3}, 12H), 1.16 (d, $^{3}J_{HH}$ = 6.6 Hz, H_{iBuCH2}, 4H), 0.75 (d, $^{2}J_{PH}$ = 13.6 Hz, 9H); ^{11}B NMR (96

MHz, C_6D_6, ppm): δ = 16.5 (bs); $^{13}C\{^1H\}$ NMR (75 MHz, C_6D_6, ppm): δ = 171.2 (d, $^2J_{PC}$ = 4.7 Hz, C_{NCO}), 143.1 (s, C_{ipso}), 129.3 (s, $C_{meta/para}$), 120.5 (s, C_{para}), 118.0 (s, $C_{meta/para}$), 35.3 (d, $^1J_{PC}$ = 115.8 Hz, C_{ylid}), 34.1 (bs, C_{iBuCH2}), 27.3 (s, C_{iBuCH3}), 26.3 (s, $C_{iBuCH1f}$), 12.6 (d, $^1J_{PC}$ = 60,7 Hz, C_{MeP}); $^{31}P\{^1H\}$ NMR (121 MHz, C_6D_6, ppm): δ = 6.2 (s); APCI-MS: decomposition; melting point: 62 °C (decomposition); elemental analysis (%): $C_{19}H_{33}BNOP$ calc. C, 68.48, H, 9.98, N, 4.20 found C, 68.31, H, 9.75, N, 4.28. IR (ATR, cm^{-1}): ũ = 2942 (vw), 2859 (vw), 1601 (vw), 1573 (vw), 1542 (vs), 1502 (m), 1449 (vw), 1419 (w), 1402 (w), 1374 (vw), 1359 (vw), 1322 (vw), 1308 (vw), 1292 (w), 1253 (vw), 1241 (w), 1165 (vw), 1108 (w), 1075 (vw), 1027 (m), 972 (s), 948 (s), 896 (vw), 880 (vw), 866 (vw), 819 (vw), 806 (vw), 752 (m), 733 (w), 692 (s), 662 (vw), 598 (vw), 570 (vw), 504 (m), 434 (vw).

6: A solution of 250 mg (1.16 mmol) **1** in 5 ml toluene was slowly added to a solution of 150 mg (1.16 mmol) PhNCS in 5 ml toluene under vigorous stirring. The solution turned slowly yellow. The solution was stirred at room temperature overnight and subsequently all volatile compounds removed in vacuo. The orange residue was solved in 2 ml toluene and layered with 15 ml pentane. After diffusion the solution was filtered off the resulting precipitate. The precipitate was washed three times, each with 15 ml pentane. The precipitate was dissolved in 1 ml toluene and layered with 15 ml pentane. After diffusion, the supernatant layer was removed and the residue was dried in vacuo. This procedure yielded 73 mg (0.21 mmol, 18%) yellow crystals: ^1H NMR (400 MHz, C_6D_6, ppm): δ = 7.57 – 7.54 (m, H_{ortho}, 2H), 7.26 – 7.21 (m, H_{meta}, 2H), 6.92 (tt, $^3J_{HH}$ = 7.5, 1.1 Hz, H_{para}, 1H), 3.55 (d, H_{ylid}, 1H), 2.37 (nonet, $^3J_{HH}$ = 6.6 Hz, $H_{Bu\text{-}CH}$, 1H), 2.35 (nonet, $^3J_{HH}$ = 6.6 Hz, $H_{Bu\text{-}CH}$, 1H), 1,40 (d, $^3J_{HH}$ = 6.3 Hz, $H_{Bu\text{-}CH2}$), 0.78 (d, $^3J_{HH}$ = 13.4 Hz, $H_{P\text{-}Me}$); ^{11}B NMR (96 MHz, C_6D_6, ppm): δ = 15.1 (s); $^{13}C\{^1H\}$ NMR (101 MHz, C_6D_6, ppm): δ = 175.8 (d, $^2J_{PC}$ = 13.6 Hz, C_{NCS}), 144.9 (s, C_{ipso}), 129.1 (s, C_{meta}), 122.8 (s, C_{para}), 122.7 (s, C_{ortho}), 49.6 (d, $^1J_{PC}$ = 122.6 Hz, C_{ylid}), 36.26 (bs, $C_{Bu\text{-}CH2}$), 27.6 (s, C_{iBuCH}), 27.2 (s, C_{iBuCH3}), 12.2 (d, $^1J_{PC}$ = 60.8 Hz, $C_{P\text{-}Me}$); $^{31}P\{^1H\}$ NMR (162 MHz, C_6D_6, ppm): δ = 5.5 (s); APCI-MS: decomposition; melting point: 89 °C (decomp.); elemental analysis (%): $C_{19}H_{33}BNPS$ calc. S 9.18; N 4.01; C 65.33; H 9.52 found S 8.78; N 4.02; C 64.98; H 9.23; IR (ATR, cm^{-1}): ũ = 2949 (w), 2911 (vw), 2863 (vw), 1594 (w), 1493 (s), 1405 (m), 1304 (m), 1260 (w), 1163 (s), 1100 (vs), 979 (vs), 905 (m), 757 (m), 740 (w), 695 (vs), 670 (w), 605 (w), 605 (w), 567 (w), 541 (w), 529 (m), 484 (s), 474 (vs), 464 (vs), 456 (vs), 444 (s), 427 (m), 414 (m), 399 (m), 388 (m), 380 (vw).

X-Ray crystallographic studies

A suitable crystal was covered in mineral oil (Aldrich) and mounted on a glass fiber or a mylar loop. The crystal was transferred directly to the cold stream of a STOE IPDS 2 diffractometer. All structures were solved by using the programs SHELXS/T[27] using Olex2.[28] The remaining non-hydrogen atoms were located from successive difference Fourier map calculations. The refinements were carried out by using full-matrix least-squares techniques on F^2 by using the program SHELXL.[29] In each case, the locations of the largest peaks in the final difference Fourier map calculations, as well as the magnitude of the residual electron densities, were of no chemical significance. Details on the data refinement are deposited in the Supporting Information.

Crystal Data **3.** $C_{25}H_{56}B_2OP_2$, M_r = 456.25, monoclinic, $P2_1/c$ (No. 14), a = 16.2691(8) Å, b = 10.2295(8) Å, c = 18.3578(10) Å, β = 92.996(4)°, $\alpha = \gamma$ = 90°, V = 3051.0(3) Å^3, T = 200 K, Z = 4, Z' = 1, $\mu(\mathrm{MoK}_\alpha)$ = 0.156, 17638 reflections measured, 17638 unique (R_{int} = 0.0237) which were used in all calculations. The final wR_2 was 0.1390 (all data) and R_1 was 0.0630 (I > 2(I)).

Crystal Data **4.** $C_{47}H_{92}B_3O_8P_3$, M_r = 910.54, triclinic, P-1 (No. 2), a = 10.3051(3) Å, b = 15.3631(5) Å, c = 18.5740(7) Å, α = 82.113(3)°, β = 82.493(3)°, γ = 79.034(3)°, V = 2843.0(2) Å^3, T = 200(2) K, Z = 2, Z' = 1, $\mu(\mathrm{MoK}_\alpha)$ = 0.148, 28135 reflections measured, 15190 unique (R_{int} = 0.0273) which were used in all calculations. The final wR_2 was 0.1634 (all data) and R_1 was 0.0523 (I > 2(I)).

Crystal Data **5.** $C_{19}H_{33}BNOP$, M_r = 333.24, monoclinic, $P2_1/n$ (No. 14), a = 11.900(2) Å, b = 13.558(3) Å, c = 12.590(3) Å, β = 95.70(3)°, $\alpha = \gamma$ = 90°, V = 2021.2(7) Å^3, T = 200 K, Z = 4, Z' = 1, $\mu(\mathrm{MoK}_\alpha)$ = 0.140, 14929 reflections measured, 5455 unique (R_{int} = 0.0579) which were used in all calculations. The final wR_2 was 0.1109 (all data) and R_1 was 0.0467 (I > 2(I)).

Crystal Data **6.** $C_{19}H_{33}BNPS$, M_r = 349.30, triclinic, P-1 (No. 2), a = 9.5890(19) Å, b = 10.106(2) Å, c = 11.551(2) Å, α = 86.62(3)°, β = 79.45(3)°, γ = 71.20(3)°, V = 1041.7(4) Å^3, T = 200 K, Z = 2, Z' = 1, $\mu(\mathrm{MoK}_\alpha)$ = 0.232, 11612 reflections measured, 5572 unique (R_{int} = 0.0360) which were used in all calculations. The final wR_2 was 0.1460 (all data) and R_1 was 0.0429 (I > 2(I)).

Crystallographic data (excluding structure factors) for the structures reported in this paper have been deposited with the Cambridge Crystallographic Data Centre as a supplementary publication no. CCDC-1920465-1920468.

Acknowledgments

We gratefully acknowledge Dr. Christopher E. Anson and M. Sc. Hanna Wagner for their help with the crystal structures. We also gratefully acknowledge M.Sc. Wolfram Feuerstein for carefully reading the manuscript.

Keywords: ylides • boranes • phosphorus • small ring systems • quantum chemistry

[1] G. H. Spikes, J. C. Fettinger, P. P. Power, *J. Am. Chem. Soc.* **2005**, *127*, 12232-12233.

[2] G. C. Welch, R. R. S. Juan, J. D. Masuda, D. W. Stephan, *Science* **2006**, *314*, 1124.

[3] a) R. L. Melen, *Science* **2019**, *363*, 479; b) M.-A. Légaré, C. Pranckevicius, H. Braunschweig, *Chem. Rev.* **2019**; c) T. Chu, G. I. Nikonov, *Chem. Rev.* **2018**, *118*, 3608-3680; d) M.-A. Légaré, G. Bélanger-Chabot, R. D. Dewhurst, E. Welz, I. Krummenacher, B. Engels, H. Braunschweig, *Science* **2018**, *359*, 896; e) S. Dagorne, R. Wehmschulte, *ChemCatChem* **2018**, *10*, 2509-2520; f) M.-A. Légaré, M.-A. Courtemanche, É. Rochette, F.-G. Fontaine, *Science* **2015**, *349*, 513; g) T. J. Hadlington, M. Driess, C. Jones, *Chem. Soc. Rev.* **2018**, *47*, 4176-4197; h) A. Merk, H. Großekappenberg, M. Schmidtmann, M.-P. Luecke, C. Lorent, M. Driess, M. Oestreich, H. F. T. Klare, T. Müller, *Angew. Chem.* **2018**, *130*, 15487-15492; i) P. P. Power, *Acc. Chem. Res.* **2011**, *44*, 627-637; j) P. P. Power, *Nature* **2010**, *463*, 171; k) S. Wang, T. J. Sherbow, L. A. Berben, P. P. Power, *J. Am. Chem. Soc.* **2018**, *140*, 590-593; l) C. Weetman, S. Inoue, *ChemCatChem* **2018**, *10*, 4213-4228.

[4] a) D. W. Stephan, *Science* **2016**, *354*; b) D. W. Stephan, G. Erker, *Angew. Chem. Int. Ed.* **2010**, *49*, 46-76; c) D. W. Stephan, *Acc. Chem. Res.* **2015**, *48*, 306-316; d) D. W. Stephan, *Dalton Trans.* **2009**, 3129-3136; e) D. W. Stephan, G. Erker, *Angew. Chem. Int. Ed.* **2015**, *54*, 6400-6441; f) J. Paradies, *Coord. Chem. Rev.* **2019**, *380*, 170-183.

[5] a) M. Melaimi, R. Jazzar, M. Soleilhavoup, G. Bertrand, *Angew. Chem.* **2017**, *129*, 10180-10203; b) G. D. Frey, V. Lavallo, B. Donnadieu, W. W. Schoeller, G. Bertrand, *Science* **2007**, *316*, 439.

[6] a) J. Escudié, C. Couret, H. Ranaivonjatovo, *Coord. Chem. Rev.* **1998**, *178-180*, 565-592; b) R. C. Fischer, P. P. Power, *Chem. Rev.* **2010**, *110*, 3877-3923; c) V. Y. Lee, A. Sekiguchi, *Organometallics* **2004**, *23*, 2822-2834; d) H. Ottosson, P. G. Steel, *Chem. Eur. J.* **2006**, *12*, 1576-1585; e) K. K. Milnes, L. C. Pavelka, K. M. Baines, *Chem. Soc. Rev.* **2016**, *45*, 1019-1035; f) J. W. Taylor, A. McSkimming, C. F. Guzman, W. H. Harman, *J. Am. Chem. Soc.* **2017**, *139*, 11032-11035; g) A.-F. Pécharman, A. L. Colebatch, M. S. Hill, C. L. McMullin, M. F. Mahon, C. Weetman, *Nat. Commun.* **2017**, *8*, 15022; h) S. J. Geier, T. M. Gilbert, D.

W. Stephan, *J. Am. Chem. Soc.* **2008**, *130*, 12632-12633; i) Z. Dong, L. Albers, M. Schmidtmann, T. Müller, *Chem. Eur. J.* **2019**, *25*, 1098-1105.

[7] a) Y. Su, Y. Li, R. Ganguly, R. Kinjo, *Angew. Chem. Int. Ed.* **2018**, *57*, 7846-7849; b) B. Wang, Y. Li, R. Ganguly, H. Hirao, R. Kinjo, *Nat. Commun.* **2016**, *7*, 11871.

[8] a) T. Tomioka, Y. Takahashi, T. Maejima, *Organic & Biomolecular Chemistry* **2012**, *10*, 5113-5118; b) T. Tomioka, R. Sankranti, T. G. Vaughan, T. Maejima, T. Yanase, *J. Org. Chem.* **2011**, *76*, 8053-8058.

[9] a) H. J. Bestmann, T. Arenz, *Angew. Chem.* **1984**, *96*, 363-364; b) O. I. Kolodiazhnyi, *Tetrahedron* **1996**, *52*, 1855-1929; for nice recent developments in ylide chemistry, see e.g.: c) L. T. Scharf, D. M. Andrada, G. Frenking, V. H. Gessner, *Chem. Eur. J.* **2017**, *23*, 4422-4434; d) T. Scherpf, K.-S. Feichtner, V. H. Gessner, *Angew. Chem. Int. Ed.* **2017**, *56*, 3275-3279; e) C. Schwarz, T. Scherpf, I. Rodstein, J. Weismann, K.-S. Feichtner, V. H. Gessner, *ChemistryOpen* **2019**, *8*, 621-626.

[10] a) M. Radius, F. Breher, *Chem. Eur. J.* **2018**, *24*, 15744-15749; for a closely related paper of our group see: b) S. Styra, M. Radius, E. Moos, A. Bihlmeier, F. Breher, *Chem. Eur. J.* **2016**, *22*, 9598-9512.

[11] H. J. Bestmann, *Chem. Ber.* **1962**, *95*, 58-63.

[12] a) H. Schmidbaur, *Acc. Chem. Res.* **1975**, *8*, 62-70; b) H. Schmidbaur, U. Deschler, B. Milewski-Mahrla, B. Zimmer-Gasser, *Chem. Ber.* **1981**, *114*, 608-619; c) H.-J. Cristau, A. Perraud, E. Manginot, E. Torreilles, *Phosphorus, Sulfur Silicon Relat. Elem.* **1993**, *75*, 7-10; d) H.-J. Cristau, *Chem. Rev.* **1994**, *94*, 1299-1313; e) H.-J. Cristau, Y. Ribeill, F. Plenat, L. Chiche, *Phosphorus, Sulfur Silicon Relat. Elem.* **1987**, *30*, 135-138.

[13] Y. Canac, C. Lepetit, M. Abdalilah, C. Duhayon, R. Chauvin, *J. Am. Chem. Soc.* **2008**, *130*, 8406-8413.

[14] H. Bohrer, N. Trapp, D. Himmel, M. Schleep, I. Krossing, *Dalton Trans.* **2015**, *44*, 7489-7499.

[15] N. Inamoto, S. Masuda, *Chem. Lett.* **1982**, *11*, 1003-1006.

[16] J. Berkowitz, G. B. Ellison, D. Gutman, *J. Phys. Chem.* **1994**, *98*, 2744-2765.

[17] H. Nöth, B. Wrackmeyer, *Chem. Ber.* **1981**, *114*, 1150-1156.

[18] a) B. M. Mikhailov, Y. N. Bubnov, *Zh. Obshch. Khim.* **1961**, *31*, 577-582; b) E. Rothgery, R. Köster, *Liebigs Ann.* **1974**, *1974*, 101-111.

[19] N. W. Mitzel, D. H. Brown, S. Parsons, P. T. Brain, C. R. Pulham, D. W. H. Rankin, *Angew. Chem. Int. Ed.* **1998**, *37*, 1670-1672.

[20] a) M. Schlosser, T. Jenny, B. Schaub, *Heteroat. Chem* **1990**, *1*, 151-156; b) S. M. Bachrach, *J. Org. Chem.* **1992**, *57*, 4367-4373.

[21] One referee of this paper suggested that the splitting in the NMR signals of **3** could also be due to *cis-trans* isomerism/bond rotation of the C–C bond of the P–C=C subunit. We thank the reviewer very much for this helpful hint. Although such an isomerism is also possible, we believe that the steric repulsion of the Me_3P and *i*Bu substituents would most likely not lead to the 1:1 intensities of the signals. We also noted that T-dependent NMR measurements at higher temperatures did not alter the 1:1 integration of the signals (see Figures S28 and S29 of the Supporting Information).

[22] G. Margraf, H.-W. Lerner, M. Bolte, *Acta Cryst. E* **2002**, *58*, o546-o547.

[23] C. Chauvier, P. Thuéry, T. Cantat, *Chem. Sci.* **2016**, *7*, 5680-5685.

[24] R. Köster, D. Simić, M. A. Grassberger, *Liebigs Ann.* **1970**, *739*, 211-219.

[25] U. Höbel, H. Nöth, H. Prigge, *Chem. Ber.* **1986**, *119*, 325-337.

[26] J. Meiners, A. Friedrich, E. Herdtweck, S. Schneider, *Organometallics* **2009**, *28*, 6331-6338.

[27] a) G. M. Sheldrick, *Crystallographic Computing 3*, **1985**; b) G. Sheldrick, *Acta Cryst. A* **2015**, *71*, 3-8.

[28] O. V. Dolomanov, L. J. Bourhis, R. J. Gildea, J. A. K. Howard, H. Puschmann, *J. Appl. Crystallogr.* **2009**, *42*, 339-341.

[29] G. Sheldrick, *Acta Cryst. C* **2015**, *71*, 3-8.

Entry for the Table of Contents (Please choose one layout)

Layout 1:

FULL PAPER

The sterically unencumbered α-borylated phosphorus ylide $Me_3PC(H)B(iBu)_2$ (**1**) has been synthesized, characterized, and investigated with the aid of density functional theory calculations. **1** has been demonstrated to react with various small molecules such as NH_3, CO, CO_2 and the heterocumulenes PhNCX. In part, different reaction products are found as compared to the previously reported derivative $Ph_3PC(Me)BEt_2$.

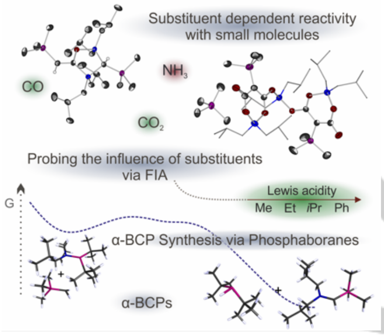

Electronic Frustration

*M. Radius, E. Sattler, H. Berberich, F. Breher**

Page No. – Page No.

Reactivity of a Sterically Unencumbered α-Borylated Phosphorus Ylide Towards Small Molecules